JOURNAL OF SOLID STATE CHEMISTRY 58, 301–311 (1985)

A Study of Polytypism in $AgIn_5Se_8$ by Combined Electron Microscopy Techniques

N. FRANGIS,*,† G. VAN TENDELOO,† C. MANOLIKAS,*
J. SPYRIDELIS,* J. VAN LANDUYT,† AND S. AMELINCKX†

*First Laboratory of Physics, University of Thessaloniki, Greece, and
†Universiteit Antwerpen, RUCA, Groenenborgerlaan 171,
B-2020 Antwerp, Belgium

Received July 6, 1984

Three different polytypes are found to exist in $AgIn_5Se_8$. They have been studied by means of conventional electron microscopy and diffraction as well as by high-resolution microscopy. The three different structures have tetragonal symmetry and can be derived from each other by means of periodic antiphase boundaries; they correspond to $c/a = 4$, $c/a = 2$, and $c/a = 1$, respectively. Regions of $c/a = 4$ often occur as microsyntactic intergrowths into $c/a = 2$ areas, and a large number of nonperiodic antiphase boundaries also occur. After fast cooling from above T_c a transition state characterized by the presence of diffuse intensity has been observed and analyzed.

1. Introduction

In the course of a systematic study of polycationic compounds with the general formula AB_5X_8 (A = Cu, Ag; B = In, Ga, Al; X = S, Se, Te) (*1*), we have studied the polytypism in $AgIn_5Se_8$ by means of electron diffraction, low-magnification diffraction contrast, and high-resolution electron microscopy.

Palatnik and Rogacheva (*2*) and Robbins and Miksovsky (*3*) have found that $AgIn_5Se_8$ has a tetragonal structure, with $c \simeq 2a$ and possible space groups $I\bar{4}$ and $I\bar{4}2m$.

Accurate X-ray analysis, performed by Benoit *et al.* (*4*), shows that the compound has a tetragonal structure with parameters $a = 5.7934$ Å and $c = 11.6223$ Å ($c/a = 2.0061$) and space group $P\bar{4}2m$. It is a superstructure based on the zincblende structure. One of the fcc sublattices is occupied by the Se atoms and the second one contains an ordered arrangement of the cations and vacancies. The Se sublattice is deformed, but the cations' sublattice is almost perfectly fcc. Figures 5a and e show the structure in space as well as the [010]-structure projection, respectively.

In the present work a second tetragonal phase of the compound was found, which has the same a parameter as the previous one, but with $c = 4a$. There is also evidence for the existence of a third phase having a cubic unit cell ($c = a$).

2. Material and Specimen Preparation

The material was prepared by mixing the appropriate quantities of Ag, In, and Se in a quartz tube which was sealed under vacuum. After the reaction of the elements, the

0022-4596/85 $3.00

material was melted and slowly cooled through the melting point.

Specimens suitable for electron microscopy studies were prepared by scraping the crystal using a knife and gluing the flakes on a grid, dipped in a Scotch tape adhesive solution. Some of the flakes were thin enough even for high-resolution observations. Specimens were also prepared by thinning disks of the material in an ion-beam thinning device.

3. Diffraction Patterns

Electron diffraction patterns reveal the existence of two tetragonal phases, with c/a ratios 2 and 4, respectively. There is also evidence for the existence of a third phase with a cubic unit cell ($c/a = 1$).

3.1. α phase ($c/a = 2$)

Diffraction patterns were obtained along a wide variety of zone axes exploring in this

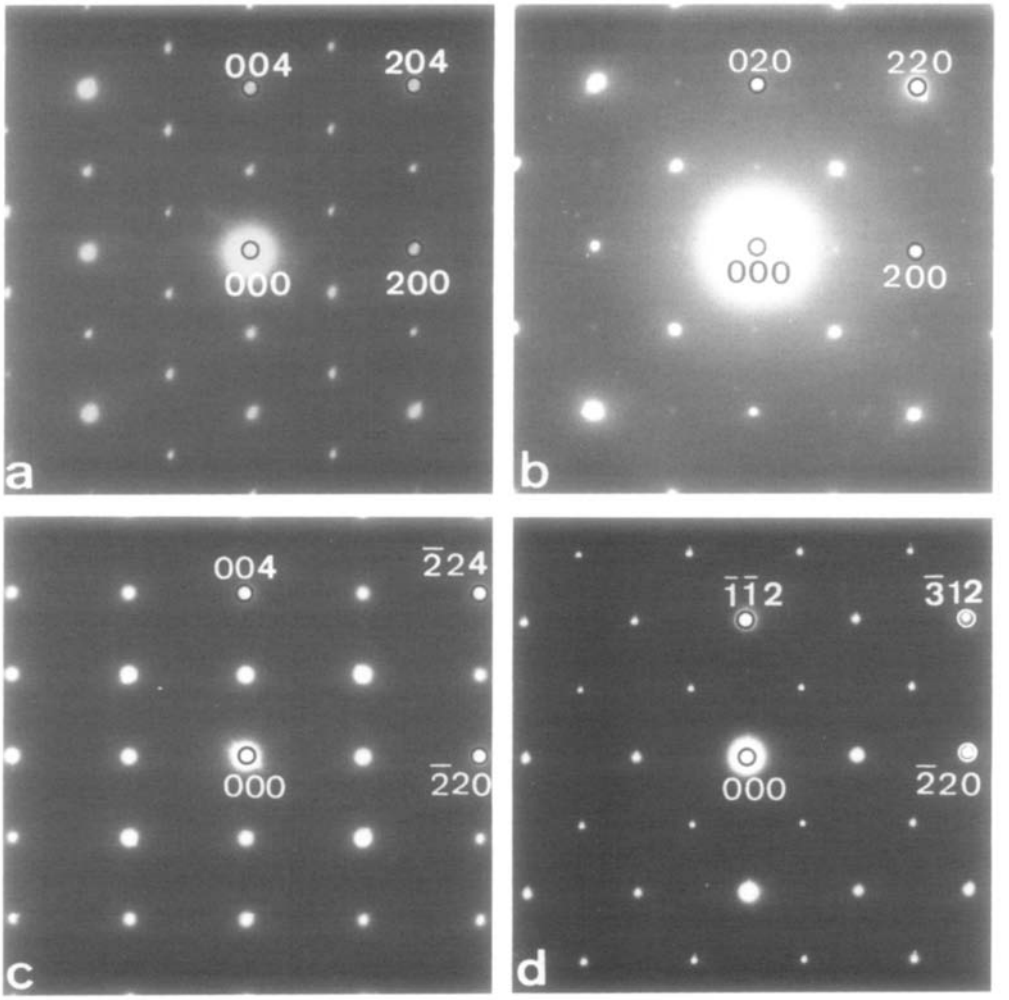

FIG. 1. Diffraction patterns reproducing several sections of the reciprocal lattice of α phase: (a) (010)*; (b) (001)*; (c) (110)*; (d) (111)*.

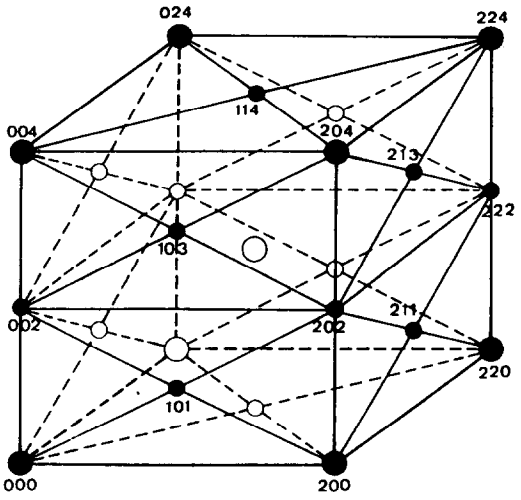

FIG. 2. The reciprocal lattice of the α phase as it is determined from diffraction patterns: large dots represent fundamental reflections; small dots represent superlattice reflections. Open circles indicate the reflections in the "invisible" part of drawing.

way the reciprocal space. Several sections of reciprocal space are reproduced in Fig. 1. The corresponding reciprocal lattice, as deduced from the experimental diffraction patterns, is a face-centered tetragonal lattice and is represented in Fig. 2. It is the same as that found in $CuIn_5Se_8$ and $CuIn_5Te_8$ (*1*).

The lattice parameters determined from the diffraction patterns ($a = a_0 \simeq 0.58$ nm and $c = 2a_0 = 1.16$ nm) are in very good agreement with those determined from X-ray diffraction (*2–4*).

Systematic extinctions were found for $h + k + l$ = odd. Although these are not consistent with the spacegroup $P\bar{4}2m$, determined in (*4*), they can be attributed to the fact that these reflections are almost entirely due to the ordering between Ag and In ($Z_{Ag} = 47$ and $Z_{In} = 49$). Their intensities are proportional to $(f_{Ag} - f_{In})^2$ which is of the order of 10^{-4} of the intensities of the ZnS-type reflections (*4*). As also mentioned by Benoit *et al.* (*4*), these reflections are absent in X-ray powder diagrams and visible only after integration of their intensities.

3.2. β phase ($c/a = 4$)

Electron diffraction patterns as in Fig. 3a reveal the existence of a second tetragonal phase with $a = a_0$ and $c' = 2c = 4a_0$. This is somewhat at variance with the results reported by Benoit *et al.* (*4*), who concluded to the existence of another tetragonal phase, called ξ phase, with $a' = \sqrt{2}a_0$ and $c'' = 4a_0$.

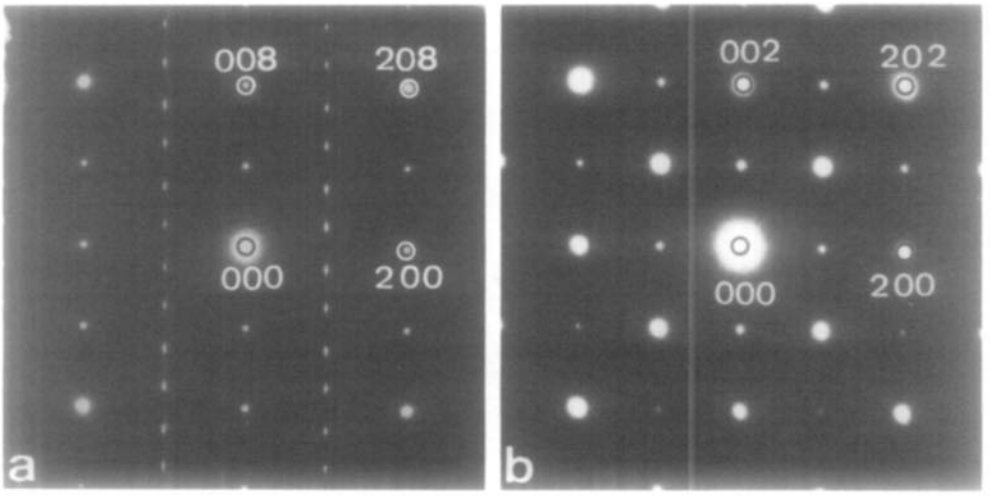

FIG. 3. (010)* diffraction patterns: (a) β phase, (b) γ phase.

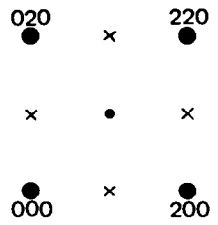

FIG. 4. The (001)* reciprocal lattice section of the α phase; small dots indicate superstructure reflections; crosses are at reflections forbidden for the α phase, but which can be present in the electron diffraction patterns due to the planar defects in (001) planes.

Except for the splitting of the spots along the [10l] row, no other extra spots occur in the diffraction patterns of β phase. Extra spots along [00l] are due to double diffraction.

3.3. γ phase ($c/a = 1$)

Diffraction patterns taken along the [001]-zone axis are expected to appear as represented in Fig. 4. In the 100 sites, indicated by crosses in the drawing, weak spots could appear because of the streaking of [10l] rows due to the isolated antiphase boundaries (APBs) perpendicular to the c

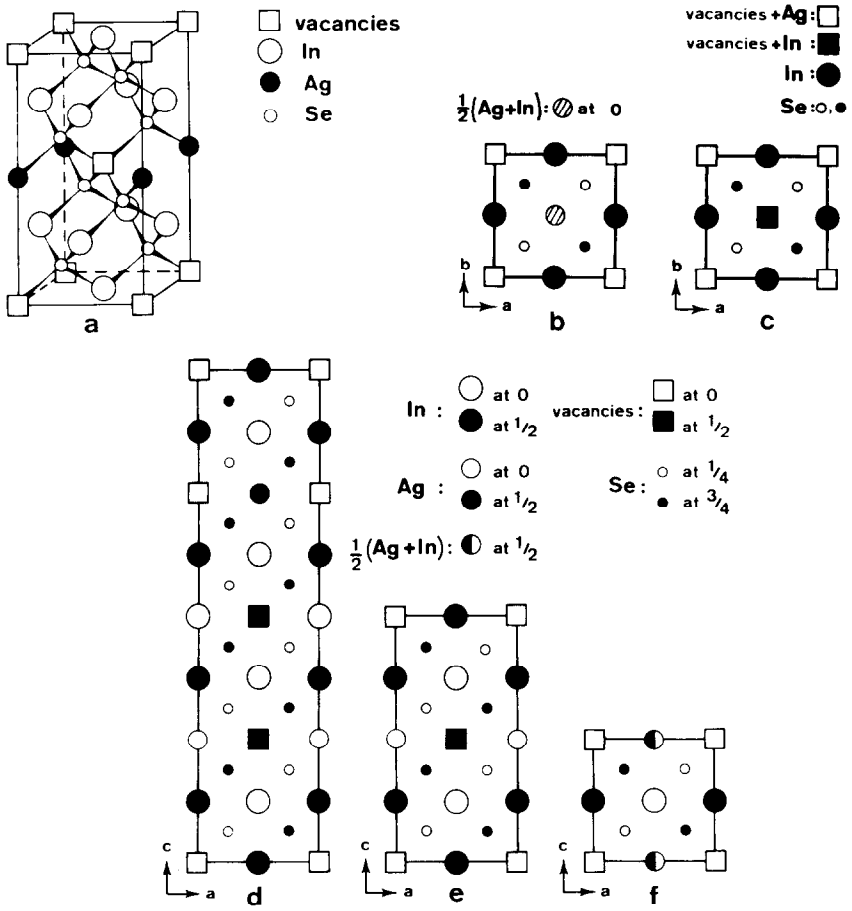

FIG. 5. (a) The α phase structure in space. (b) The (001)-structure projection of the γ phase. (c) The (001)-structure projection of the α phase. (d, e, f) The (010)-structure projections of β, α, and γ phases, respectively. The labels indicated on top of (c) are valid only for this figure. For (b), (d), (e), and (f) the conventions on top of (e) and (f) have been used.

axis (see Fig. 1a and also 3a). Such a pattern is shown in Fig. 1b. But in some patterns, relatively strong reflections appear in the 100 positions, which from the general aspect of the diffraction pattern cannot be interpreted as being due to the streaking (Fig. 3b). The most probable explanation is that a third phase exists, which is at least tetragonal. Dark-field images taken in 100 spots reveal bright but small areas in the whole matrix, substantiating the existence of this third phase. In the related compound CdI_2Se_4 three phases exist with c/a ratios *1*, *2*, and *4* (*5*). Therefore the third phase in $AgIn_5Se_8$ most probably has also a cubic unit cell but only tetragonal symmetry (space group $P\bar{4}2m$). This allows us to interpret the diffraction patterns as well as the high-resolution images.

4. Models for the Structures

The structure of the γ phase is related to that of $CdIn_2Se_4$, by statistically distributing $\frac{1}{2}$(Ag + In) instead of Cd. The [010]-structure projection is shown in Fig. 5f.

The α phase can be derived from the γ phase by introducing periodic antiphase boundaries parallel to (001) planes, with period a_0 and displacement vector $\mathbf{R} = \frac{1}{2}[110]$. To be consistent with the structure determined by Benoit *et al.* (*4*), we have to accept ordering between Ag and In and a distortion of the Se sublattice.

The β phase can be derived similarly by introducing in the γ phase the same type of APB, but with a period $2a_0$. Also it can be considered to be derived from the α phase. Its [010]-structure projection is shown in Fig. 5d.

The interpretation based on the periodic introduction of APBs is substantiated by the following observations:

(1) Isolated antiphase boundaries are observed, in the α and β phases, perpendicular to c axis and with $\mathbf{R} = \frac{1}{2}[11w]$.

(2) High resolution images clearly show the existence of one phase as bands within the other one (Fig. 6). Also a band (δ) with a

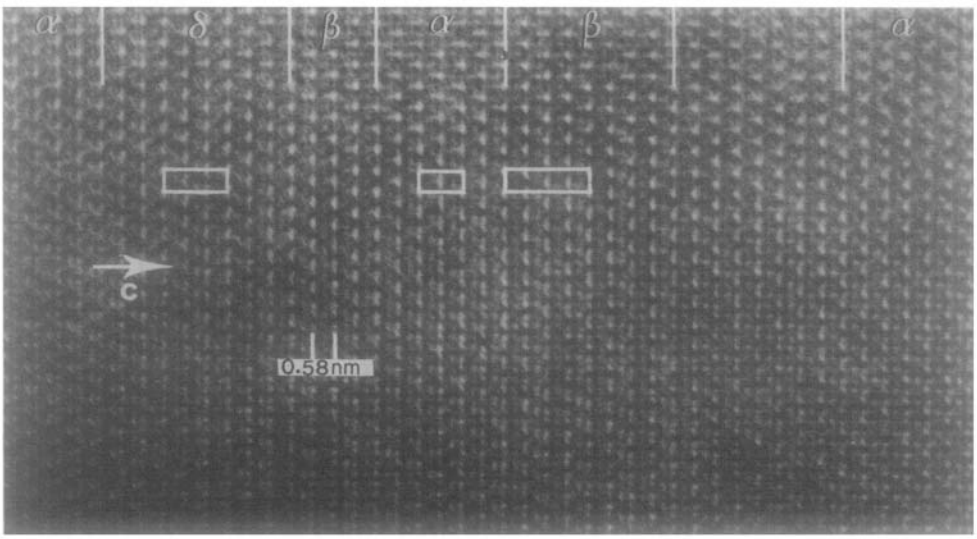

FIG. 6. Part of a crystal of $AgIn_5Se_8$ in the (010) projection containing APB's, which locally create bands of α and β phase, as well as band with a period $c = 3a_0$ (indicated by δ). The unit cells are shown in every region. The configuration of the bright spots corresponds in each case to the vacancy configuration in the (010)-structure projection.

$c = 3a_0$ structure is locally created over a very small width.

A similar interpretation was also proposed for the occurrence of the different structure types in $CdIn_2Se_4$ (*5*).

5. The Domain Structure

5.1. Group Theoretical Considerations

We will only discuss the α phase, since this is the only one of which we know exactly the space group. As it is described in (*2*) this phase undergoes a phase transition whereby cations and vacancies disorder on their sublattice. The disordered phase is a zincblende-like structure with lattice parameter $a = a_0$. Its pointgroup is $\bar{4}3m$ of order 24; that of the ordered phase is $\bar{4}2m$ of order 8. A variant generating group is thus

$$V = 3 = \{E, C_3^1, C_3^2\}$$

which is of order 3 (*6*).

Three orientation variants are thus expected in the α phase, which are related one to the other by 120° rotations about the threefold axis. It means that the three orientation variants have their c axes mutually perpendicular and parallel to the three possible cube directions. To find the number of translation variants we consider the transformation between the ordered and disordered phase (*6*), which is

$$M = \begin{pmatrix} 1 & 0 & 0 \\ 0 & 1 & 0 \\ 0 & 0 & 2 \end{pmatrix}.$$

Since the ordered unit cell is primitive and the disordered one fourfold, the total number of translation variants is

$$t = \tfrac{4}{1}|M| = 8.$$

By comparison of the two unit cells the seven displacement vectors between the translation variants can be deduced as

$$\mathbf{r}_1 = \tfrac{1}{2}[110], \quad \mathbf{r}_2 = \tfrac{1}{4}[201],$$
$$\mathbf{r}_3 = \tfrac{1}{4}[021], \quad \mathbf{r}_4 = \tfrac{1}{2}[001],$$
$$\mathbf{r}_5 = \tfrac{1}{4}[023], \quad \mathbf{r}_6 = \tfrac{1}{4}[203],$$
$$\mathbf{r}_7 = \tfrac{1}{2}[111].$$

It is clear that for the β phase, at least these three orientation variants are expected since the three cube directions have equal probability to become the c axis of the tetragonal structure.

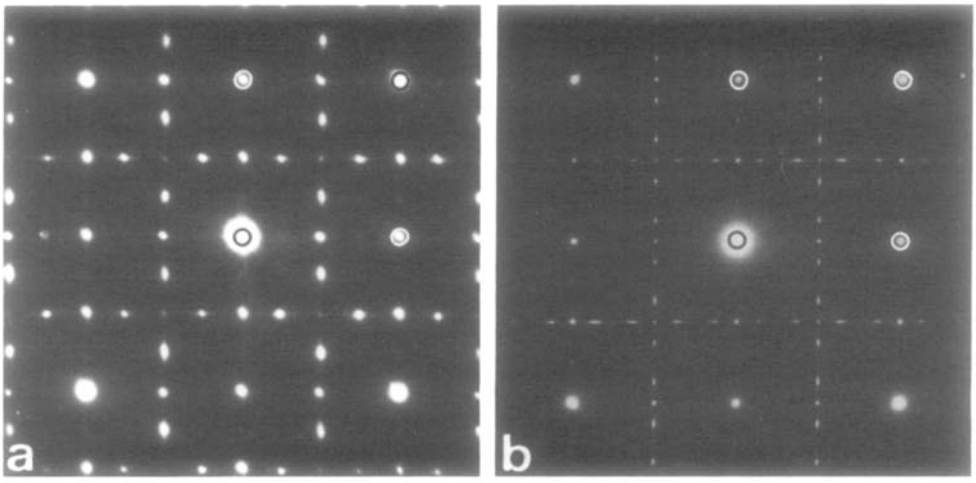

FIG. 7. Cube-zone diffraction patterns of areas containing three orientation variants: (a) α phase, (b) β phase. Very weak spots in (a) are due to double diffraction.

5.2. Observation of the Domain Structure

The existence of the three orientation variants in the same area is revealed by the diffraction patterns which can be interpreted by the assumption of the coexistence of the three variants. Such patterns for the α and β phases are shown in Fig. 7. Dark-field images taken with spots from the subpatterns substantiate this interpretation. An example is shown in Figs. 8a–c. The orientation of the c axis is indicated for each variant.

Both the a and the b phases exhibit a large number of antiphase boundaries, as can be judged from Fig. 8d. These are also visible in two of the variants of Fig. 8 as well as in high-resolution images such as Fig. 9a. Their planes are perpendicular to the c axis. Extinction contrast experiments show that their displacement vector is $\mathbf{R} = \frac{1}{2}[11w]$, i.e., $\mathbf{R} = \mathbf{r}_1$ or $\mathbf{R} = \mathbf{r}_7$. Neither dis-

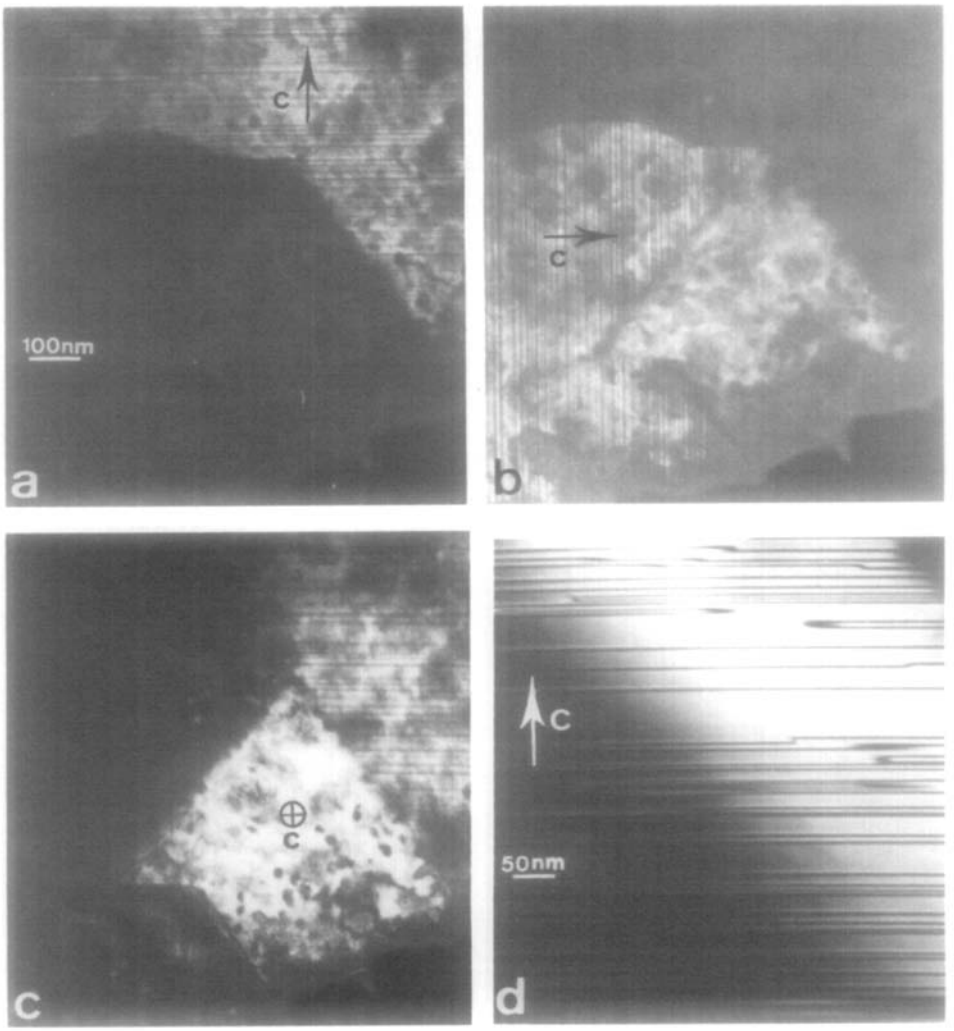

FIG. 8. (a–c) Domain structure in $AgIn_5Se_8$. Dark-field images taken in spots belonging to three different orientation variants. (d) Antiphase boundaries present in one variant reproduced at a higher magnification. Note the presence of hairpins.

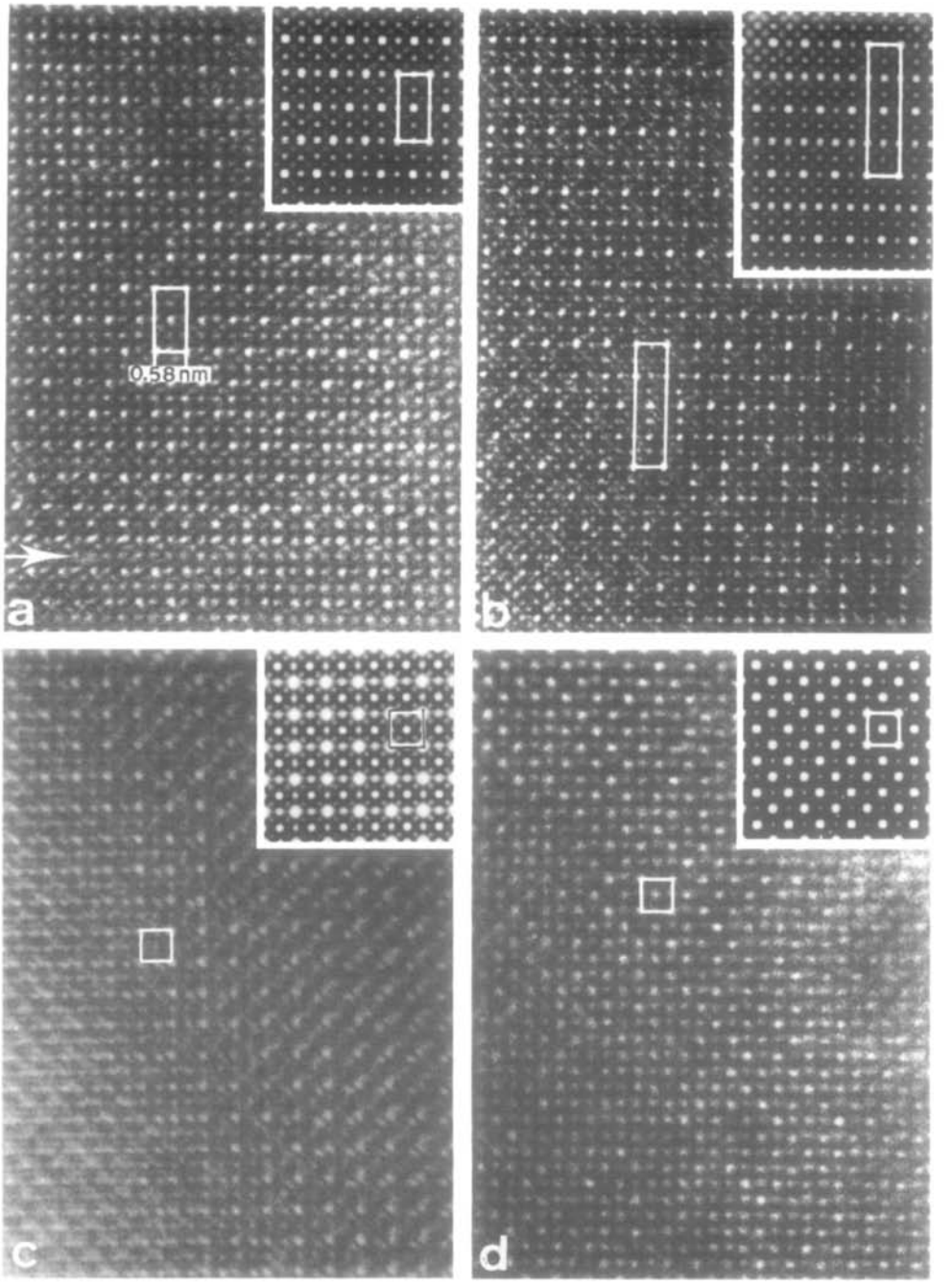

FIG. 9. High-resolution images in $AgIn_5Se_8$. The corresponding calculated images are shown as insets. The images were taken along the axes: (a) [010] of the α phase (thickness: 9.3 nm, $\Delta f = -100$ nm); (b) [010] of the β phase (thickness: 9.3 nm, $\Delta f = -100$ nm); (c) [001] of the γ phase (thickness: 13.9 nm, $\Delta f = -47.5$ nm), (d) [001] of the α phase (thickness: 11.6 nm, $\Delta f = -110$ nm). The unit cells are shown in each case. In (a) an APB is indicated by an arrow.

placement vector can be discerned from either diffraction contrast experiments or from the high-resolution images.

The existence of these APBs explains the fact that the distances between the spots along the [10l] row in the diffraction pattern of Figure 3a are not equal to each other (incommensurate phase). According to Fujiwara (*7*) maxima of intensity are expected for $l = 1/2M$ and $1 - 1/2M$ (cubic indexation), where M (in a_0) is the mean period of APBs. For the diffraction pattern of Fig. 3a a value of $M = 1.88$ was found instead of $M = 2$ for the perfect structure.

High-resolution images of the γ phase reveal the existence of two kinds of APBs, in planes perpendicular to each other and with possible displacement vectors $\frac{1}{2}[110]$, $\frac{1}{2}[101]$, and $\frac{1}{2}[011]$.

6. High-Resolution Images

The analysis of this phase was complemented by high-resolution observations for several situations:

(1) along the [100]- and [001]-zone axes of the α phase (Figs. 9a and d);

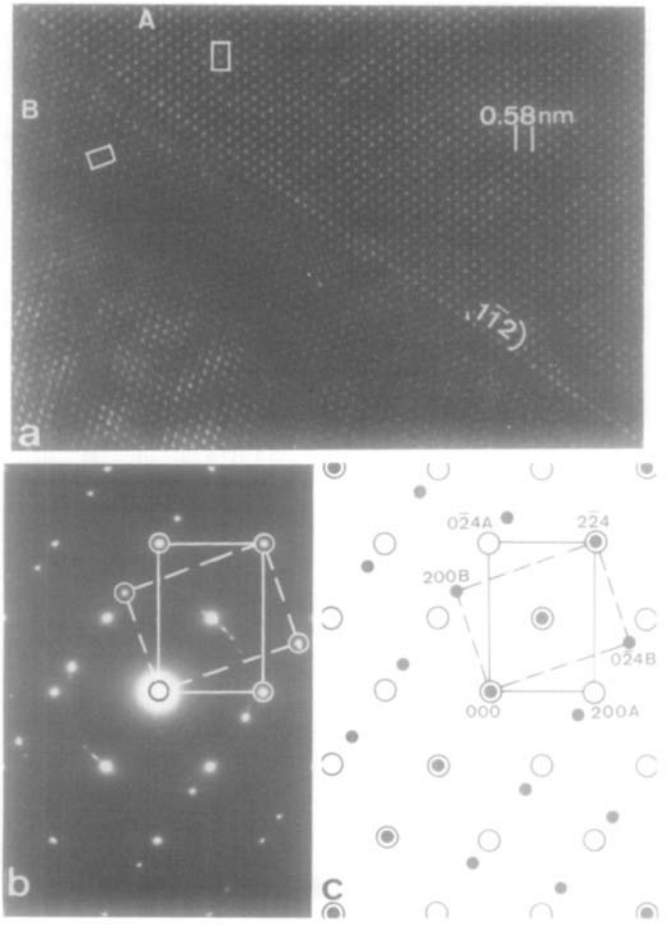

FIG. 10. (a) Twinning in $AgIn_5Se_8$. (b) Corresponding (021)* diffraction pattern. (c) Schematic representation of the diffraction pattern. Open and filled circles represent spots coming from the two parts of the crystal.

(2) along the [100]-zone axis of the β phase (Fig. 9b);

(3) along the [001]-zone axis of the γ phase (Fig. 9c).

In all figures the corresponding calculated images are shown as insets. For the calculations the model for the α phase proposed by Benoit *et al.* (*4*) was used and the models proposed in the present paper for the β and γ phases. Calculations were performed for a spherical aberration constant C_s = 1.2 mm and the defocus spread = 3 nm.

The very good resemblance between the experimental and the calculated images, as well as with the corresponding structure projections (Fig. 5) supports the validity of the proposed models.

7. Twinning

Evidence was also found for twinning in the crystals of $AgIn_5Se_8$. From the analysis of the diffraction patterns it can be deduced that they are reflection twins on the $(1\bar{1}1)$ plane of the fcc sublattice (equivalent $(1\bar{1}2)$ of the α phase). It is a twinning mode frequently occurring in the fcc crystals (*8*).

A high-resolution image taken along the [021] axis reveals the existence of twinned crystal parts related by the above mentioned operation (Fig. 10a). The diffraction pattern from an area as shown in this figure is represented as Fig. 10b. It can be interpreted easily as the superposition of two diffraction patterns taken along the [021] axis and related one to the other by reflection with respect to the $[1\bar{1}2]^*$ direction. Figure 10c illustrates this interpretation [see also (*8*)].

8. The "Disordered" Phase

As mentioned in (*2*), above 685°C a disordered cubic phase exists. Upon heating the crystal in the electron microscope the superstructure spots disappear and after cooling an extended diffuse intensity is observed (Fig. 11a). A similar diffuse intensity but even more pronounced has been observed in $CuIn_5Se_8$ and in $CuIn_5Te_8$ (*1*).

Since the basic fcc reflections remain sharp it is assumed that the Se sublattice remains undisturbed and that the disordering or short-range ordering only affects the cation sublattice. The exact shape of this diffuse intensity will be treated in more detail in (*9*) but to a first approximation it con-

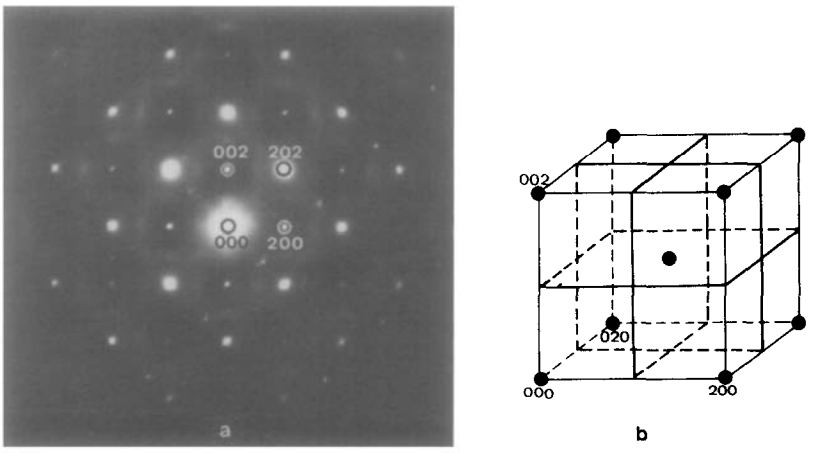

FIG. 11. Transition state: (a) Experimental (010)* diffraction pattern (indices refer to the fcc lattice). (b) The locus of diffuse intensity in reciprocal space.

sists of lines of diffuse intensity parallel to the cube directions, e.g., $h = 2n + 1, k = 2n$ ($l = 2n$) (Fig. 11b). It was shown in (*10*) that this locus corresponds to a transition state characterized by a tetrahedral cluster of cations having the macroscopic 3 : 1 composition (three cations and one vacancy).

9. Conclusions

Electron diffraction patterns and high resolution images confirm the existence of three tetragonal polytypes in $AgIn_5Se_8$. For the *a* and *b* phase the *c*/*a* ratios are 2 and 4, respectively. The γ phase has most probably a cubic unit cell (*c*/*a* = 1). It has not been possible to determine its symmetry unambiguously.

The models of periodic APBs for the description of the structure are in good agreement with the high-resolution images.

The domain structure and the transition state are similar to the ones observed in the other related compounds (*1*).

References

1. C. MANOLIKAS, J. VAN LANDUYT, R. DE RIDDER, AND S. AMELINCKX, *Phys. Status Solidi A*, **55,** 709 (1979); C. MANOLIKAS, R. DE RIDDER, J. VAN LANDUYT, AND S. AMELINCKX, *Phys. Status Solidi A*, **59,** 621 (1980); N. Frangis, C. Manolikas, and J. Spyridelis, *Mater. Res. Bull.* **17,** 1089 (1982).
2. L. S. PALATNIK AND E. I. ROGACHEVA, *Sov. Phys. Crystallogr. Engl. Transl.* **11,** 189 (1966).
3. M. ROBBINS AND M. A. MIKSOVSKY, *Mater. Res. Bull.* **6,** 359 (1971).
4. P. BENOIT, P. CHARPIN, AND C. DJEGA-MARIADASSOU, *Mater. Res. Bull.* **18,** 1047 (1983).
5. C. MANOLIKAS, D. BARTZOKAS, G. VAN TENDELOO, J. VAN LANDUYT, AND S. AMELINCKX, *Phys. Status Solidi A*, **59,** 425 (1980).
6. G. VAN TENDELOO AND S. AMELINCKX, *Acta Crystallogr. A* **30,** 341 (1974).
7. K. FUJIWARA, *J. Phys. Soc. Japan*, **12,** 7 (1957).
8. J. W. EDINGTON, "Electron Diffraction in the Electron Microscope," p. 46, McMillan Philips Technical Library (1975).
9. N. FRANGIS *et al.*, to be published.
10. R. DE RIDDER, G. VAN TENDELOO, AND S. AMELINCKX, *Acta Crystallogr. A* **32,** 216 (1976).